Accepted Manuscript

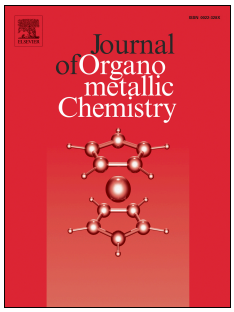

Mixed ligand ruthenium arene complexes containing N-ferrocenyl amino acids: Biomolecular interactions and cytotoxicity against MCF7 cell line

Pulipaka Ramadevi, Rinky Singh, Sarmita S. Jana, Ranjitsinh Devkar, Debjani Chakraborty

PII: S0022-328X(17)30049-9

DOI: 10.1016/j.jorganchem.2017.01.020

Reference: JOM 19777

To appear in: *Journal of Organometallic Chemistry*

Received Date: 27 July 2016

Revised Date: 29 December 2016

Accepted Date: 30 January 2017

Please cite this article as: P. Ramadevi, R. Singh, S.S. Jana, R. Devkar, D. Chakraborty, Mixed ligand ruthenium arene complexes containing N-ferrocenyl amino acids: Biomolecular interactions and cytotoxicity against MCF7 cell line, *Journal of Organometallic Chemistry* (2017), doi: 10.1016/j.jorganchem.2017.01.020.

Mixed ligand Ruthenium arene complexes containing N-Ferrocenyl amino acids: Biomolecular interactions and Cytotoxicity against MCF7 cell line

Pulipaka Ramadevi [1], Rinky Singh[1], Sarmita S Jana[2], Ranjitsinh Devkar[2] and Debjani Chakraborty[1*]

[1]Department of Chemistry, Faculty of Science, The M.S. University of Baroda, Vadodara-390002, Gujarat. INDIA.

[2]Division of Phytotherapeutics and Metabolic Endocrinology, Department of Zoology, Faculty of Science, The M.S. University of Baroda, Vadodara-390002, Gujarat. INDIA.

*Corresponding author. Tel.:+91 9537521703, E-mail address: debchak23@gmail.com

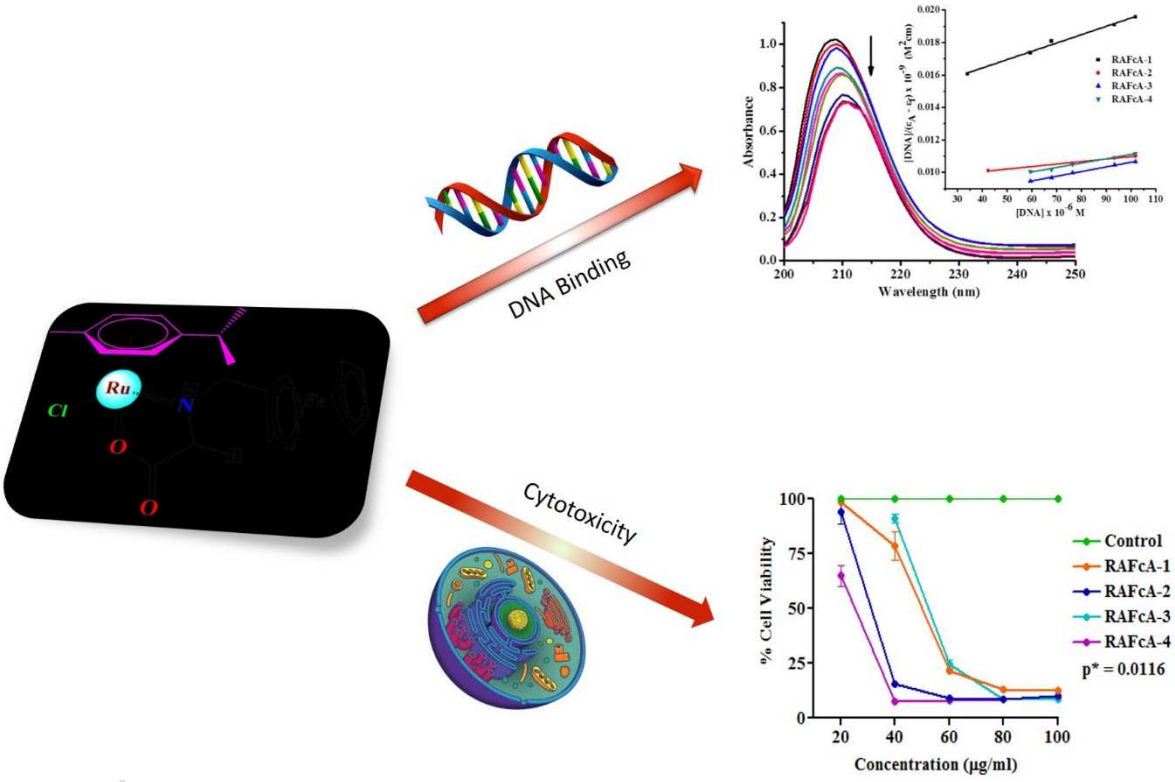

Mixed ligand Ruthenium arene complexes containing N-Ferrocenyl amino acids: Biomolecular interactions and Cytotoxicity against MCF7 cell line

Pulipaka Ramadevi [1], Rinky Singh[1], Sarmita S Jana[2], Ranjitsinh Devkar[2] and Debjani Chakraborty[1*]

[1]Department of Chemistry, Faculty of Science, The M.S. University of Baroda, Vadodara-390002, Gujarat. INDIA.

[2]Division of Phytotherapeutics and Metabolic Endocrinology, Department of Zoology, Faculty of Science, The M.S. University of Baroda, Vadodara-390002, Gujarat. INDIA.

*Corresponding author. Tel.:+91 9537521703, E-mail address: debchak23@gmail.com

Abstract

Synthesis, characterization, DNA and protein binding as well as anticancer activity of the organometallic complexes [Ru(η^6-*p*-cym)(L)Cl] (where, *p-cym* = *p*-cymene $MeC_6H_4Pr^i$, L = N-ferrocenyl amino acid conjugates) **RAFcA 1-4** have been described. The complexes **1-4** exhibited strong DNA/BSA binding and anticancer activity against breast cancer MCF7 cell line. Their binding with calf thymus DNA (CT DNA) and bovine serum albumin (BSA) have been examined by absorption and emission spectral studies. Strong interactions between complexes and CT-DNA have been affirmed by absorption spectral and EB displacement studies, while interaction with BSA via static quenching was explored by fluorescence titration. Cytotoxicity, apoptosis and in vitro anticancer activity of **1-4** toward MCF7 cell line have been investigated by MTT assay. The IC_{50} values (37.1μM - 86.6μM) were found to be distinctly lower than those of NAMI-A and RAPTA complexes for MCF7 cell line which was followed by gene expression studies to confirm apoptosis as the mode of cell death.

Keywords

N-Ferrocenyl amino acids, ruthenium arene complexes, DNA/BSA binding interactions, MCF7 human breast carcinoma, apoptosis**.**

1. Introduction

Ferrocene is one of the members of the well known organometallic family- "metallocenes" in which an iron atom is flanked by two cyclopentadienyl (Cp) rings. The unique structural and conformational properties of ferrocene are characterized by the parallel alignment of the two cyclopentadienyl rings and the free rotation of the rings around the axis penetrating their centers. Its remarkable stability and fascinating chemistry has attracted the attention of the scientific and technical community. Owing to the favourable electronic properties of ferrocene and its easy functionalization their applications have been explored in a wide range of scientific areas ranging from catalysis to the design of new nonlinear optic materials to new biologically active compounds. Several structural modifications of established drugs with ferrocenyl moiety have been reported, such as ferrocene fluconazole [1], ferrocene aspirin [2], mefloquine [3] and artemisinin [4]. Moreover ferrocene derivatives have been used as scaffolds to design new molecules that recognize cations, anions, organic molecules, nucleobases, dinucleotides and amino acids [5-10]. Mitsuo Sekine *et al* [11] have reported new DNA binding molecules utilizing structural and conformational properties of ferrocene. Their design concept is based on the fact that the distance between the two cyclopentadienyl rings of ferrocene, ca. 3.3 Å is close to the distance between two aromatic rings stacked with each other. In addition, it is well-known that the minor groove of DNA can accommodate stacked aromatic rings, as established by the structural studies of natural or synthetic molecules that recognize the minor groove. Therefore, it was expected that ferrocene derivatives could be a new type of DNA binding molecules if appropriately designed aromatic rings were attached to the Cp rings. Recent studies on interaction of ferrocenyl ligands with DNA has shown binding constants to be in the order of 10^3-10^5 [12] agreeing with the above mentioned fact. The stability of ferrocene in aqueous and aerobic media has made ferrocenyl compounds very popular molecules for such biological applications. Furthermore such favorable characteristics of ferrocene led to the design of ferrocenyl derivatives that function as highly sensitive detectors of proteins or as reporters of protein activity. Studies on ferrocenyl conjugates with amino acids and end-labeled ferrocenyl di- and tripeptides have demonstrated distinctive electrical, structural, and medicinal properties [13]. Many researchers have shown interest in design of unnatural ferrocenyl amino acids and peptides which further have been studied for their biomedical applications. Modification of proteins by

incorporating such unnatural ferrocenyl amino acids helps the study of protein structure, activity and interaction with other biomolecules [14].

The ferrocenyl compounds are known to hold good potential as anticancer agents. This can be exemplified by the results obtained by the group of Gérard Jaouen, with the development of ferrocifens (i.e. ferrocene-modified tamoxifens), which exhibit strong antiproliferative effects not only in hormone dependent but also in hormone-independent breast cancer cells [15]. A recent review by Ca´tia Ornelas throws light on the various applications of ferrocene and its derivatives in cancer research [16].

The field of antitumoural and antimetastatic arene ruthenium complexes was pioneered by P.J.Dyson and by P.J.Sadler, [17,18] after the notion of using arene ruthenium compounds as anticancer agents had first been introduced by Tocher *et al.* in 1992, who had observed a cytotoxicity enhancement by coordinating the anticancer agent metronidazole [1-β-(hydroxyethyl)-2-methyl-5-nitro-imidazole] to a benzene ruthenium dichloro fragment [19]. Since arenes are known to stabilise ruthenium in its 2+ oxidation state, investigations have been done into the potential of Ru(II) arene complexes as anticancer agents. It is found that in such ‘‘half-sandwich’’ Ru(II) mono-arene complexes, the arene ligand is relatively inert towards displacement under physiological conditions. There is a delicate balance between electron donation from the arene into the empty ruthenium 4d orbitals and back-donation from the filled $4d^6$ orbitals into vacant arene orbitals. This is influenced by the donor–acceptor power of the arene (e.g. hexamethylbenzene as a strong donor, in contrast to biphenyl which may act as acceptor) and by the other ligands on Ru(II) which can influence the availability of the $4d^6$ electrons, e.g. presence of strong π-acceptor chelating ligands such as bipyridine and azopyridine [20], or donor strength of mondentate ligands (e.g. iodide vs. chloride) [21]. In this context, very recently, attention has been focused on organometallic Ru(II) arene complexes and their anticancer activities have been studied by varying the arene, substituent ligand and leaving group [22]. These ‘piano-stool’ frameworks provide a handle for optimizing the design of drugs in terms of pharmacological properties and reducing the side effects.

Here we are reporting a series of mixed ligand ruthenium(II) complexes bearing amino acid conjugated ferrocenyl compounds and *p*-cymene as the ancillary arene ligand. These ferrocenyl amino acids have been targeted as it has been shown that tethering biologically active groups to the ferrocenyl unit increases their potency, possibly due to the combined action of the organic molecule with Fenton chemistry of the Fe-centre

[23, 24]. Since DNA represent very important potential target of cancer diagnostic and chemotherapy drugs, before going to expensive cell line study it was decided to preliminarily explore the anticancer potency of the compounds by determining their DNA interaction because 'the control over DNA can control the cancerous cell growth'. Like DNA, proteins are also considered to be one of the prime molecular targets for diagnostic and imaging agents, and so equal attention has been paid on designing novel probes for proteins [25-27].

The ferrocene amino acid derivatives have been coordinated to $[Ru(\eta^6\text{-}p\text{-cym})Cl]^+$ and investigated for their interaction with DNA and BSA (bovine serum albumin). Results obtained from the binding studies prompted the *in-vitro* cytotoxicity evaluation of ruthenium complexes on MCF7 human breast carcinoma cells using MTT assay. The interaction of these complexes with MCF7 cells has been scrutinized using gene expression assay employing RT-PCR technique to assess the mechanism of cell death *viz.* apoptotic or necrotic.

2. Experimental

2.1. *Reagents and materials*

All the chemicals and solvents used for synthesis and characterization of ligands and complexes are of analytical grade and were used as purchased. Synthesis of ferrocenyl amino acid conjugates (**FcA 1-4**) has been previously reported by our group [28]. The precursor $[Ru(\eta^6\text{-}p\text{-cymene})Cl_2]_2$ was prepared according to the procedure sited in literature [29]. α-terpinene was purchased from Sigma-Aldrich. $RuCl_3.3H_2O$ was purchased from Hi-media. CT-DNA, Tri-sodium citrate and EB (ethidium bromide) were purchased from SRL (Sisco research laboratory, Mumbai, India.). BSA (bovine serum albumin) was purchased from Hi media (Mumbai, India). All the solvents used in the present studies were purchased from Merck and are of analytical grade.

2.2. *Methods and instrumentation*

ESI Mass spectra were recorded on Applied Biosystem API 2000 Mass spectrometer. Infrared spectra ($400\text{-}4000cm^{-1}$) were recorded on Perkin Elmer RX-1 FTIR with samples prepared as KBr pellets. UV spectra were recorded in DMSO solution at concentrations in the range 10^{-6}–10^{-3}M on Perkin Elmer Lambda-35 dual beam UV-Vis spectrophotometer. Fluorescence spectra were recorded in solution on JASCO FP-6300 fluorescence spectrophotometer.

2.3. *Synthesis of [Ru(η6-p-cym)(FcA)Cl] complexes (**RAFcA 1-4**)*

[Ru(η^6-*p*-cym)(FcA)Cl] **(RAFcA 1-4)** were prepared by a typical µ-chlorido-bridge splitting reaction of [Ru(η^6-*p*-cymene)Cl_2]$_2$. To a solution of [Ru(η^6-*p*-cymene)Cl_2]$_2$ (in 2.5 ml CH_2Cl_2), the synthesized ligand **FcA** (in 2.5 ml methanol) was added on stirring in 1:2 mole ratio respectively. The reaction mixture was left on stirring overnight (20-24 h) at room temperature. The reaction mixture was then left for slow evaporation at r.t. The resultant reddish brown crystalline solid was then filtered, washed with pet ether and CH_2Cl_2 and dried in oven at 40°C for 1 h. The complexes so obtained were recrystallized from dichloromethane and ether which resulted in reddish brown crystals but not of the single crystal quality. **Fig. 1** shows the general synthetic route for the preparation of **RAFcA 1-4** complexes.

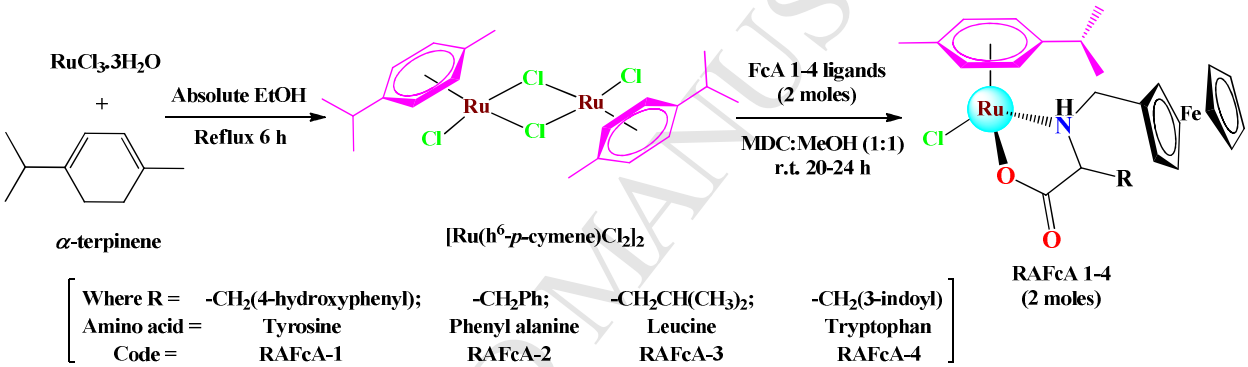

***Fig. 1:** General synthetic scheme of **RAFcA 1-4** complexes.*

[Ru(η^6-p-cym)(FcA-1)Cl] **(RAFcA-1)**:

RAFcA-1 was synthesized by reaction of [Ru(η^6-*p*-cymene)Cl_2]$_2$ (0.049 mmol, 30.0 mg) and ligand **FcA-1** (0.098 mmol, 37.1 mg). Soluble in almost all organic solvents like DMSO, MeOH, CH_2Cl_2. Yield: 69.1%; Molecular Weight 648.97 g/mole; Molecular Formula $C_{30}H_{35}ClFeNO_3Ru$; Anal. Found: C, 55.09; H, 5.31; N, 2.20. Calc.: C, 55.44; H, 5.43; N, 2.15. ESI-MS *m/z*: 650.1 (M^++1), 614.1 (M^+-Cl); δ_H (400 MHz, DMSO-d_6): 10.78 (s, 1H, OH of phenylalanine), 7.63-8.01 (m, 5H, Ar-H of phenylalanine), 5.81-5.75 (m, 4H, *p*-cym Ar-H), 4.59 (t, 2H, substituted cyclopentadiene), 4.33 (t, 2H, substituted cyclopentadiene), 4.15 (s, 5H, cyclopentadiene), 2.81 (q, 1H, *p*-cym-*iso*-prop-CH), 2.06 (s, 3H, *p*-cym Ar-CH_3), 1.19 (d, 6H, *p*-cym-*iso*-prop-$(CH_3)_2$); FTIR (KBr/ cm^{-1}): $\nu_{(Ar)C-H}$ 2959, $\nu_{COOassym}$ 1580, ν_{COOsym} 1392, $\Delta\nu_{COO}$ 188.

[Ru(η^6-p-cym)(FcA-2)Cl] **(RAFcA-2)**:

RAFcA-2 was synthesized by reaction of [Ru(η^6-*p*-cymene)Cl_2]$_2$ (0.049 mmol, 30.0 mg) and ligand **FcA-2** (0.098 mmol, 35.6 mg). Soluble in almost all organic solvents like DMSO, MeOH, CH_2Cl_2. Yield: 74.3%; Molecular Weight 633.97 g/mole; Molecular Formula $C_{30}H_{35}ClFeNO_2Ru$; Anal. Found: C, 56.21; H, 5.17; N, 2.10. Calc.: C, 56.84; H, 5.56; N, 2.21. ESI-MS *m/z*: 633.9 (M^+), 597.9 (M^+-Cl); δ_H (400 MHz, DMSO-d_6): 7.10-7.38 (m, 5H, Ar-H of tyrosine), 5.81-5.25 (m, 4H, *p*-cym Ar-H), 4.82 (t, 2H, substituted cyclopentadiene), 4.57 (t, 2H, substituted cyclopentadiene), 4.19 (s, 5H, cyclopentadiene), 2.81 (q, 1H, *p*-cym-*iso*-prop-CH), 2.08 (s, 3H, *p*-cym Ar-CH_3), 1.19 (d, 6H, *p*-cym-*iso*-prop-$(CH_3)_2$); FTIR (KBr/ cm^{-1}): $\nu_{(Ar)C-H}$ 2959, $\nu_{COOassym}$ 1626, ν_{COOsym} 1371, $\Delta\nu_{COO}$ 255.

[Ru(η^6-p-cym)(FcA-3)Cl] **(RAFcA-3)**:

RAFcA-3 was synthesized by reaction of [Ru(η^6-*p*-cymene)Cl_2]$_2$ (0.049 mmol, 30.0 mg) and ligand **FcA-3** (0.098 mmol, 32.3 mg). Soluble in almost all organic solvents like DMSO, MeOH, CH_2Cl_2. Yield: 77.9%; Molecular Weight 599.96 g/mole; Molecular Formula $C_{27}H_{37}ClFeNO_2Ru$; Anal. Found: C, 53.55; H, 6.08; N, 2.09. Calc.: C, 54.05; H, 6.22; N, 2.33. ESI-MS *m/z*: 599.9 (M^+), 563.9 (M^+-Cl); δ_H (400 MHz, DMSO-d_6): 5.82-5.77 (m, 4H, *p*-cym Ar-H), 4.36 (t, 2H, substituted cyclopentadiene), 4.20 (t, 2H, substituted cyclopentadiene), 4.15 (s, 5H, cyclopentadiene), 2.75 (q, 1H, *p*-cym-*iso*-prop-CH), 2.03 (s, 3H, *p*-cym Ar-CH_3), 1.19 (d, 6H, *p*-cym-*iso*-prop-$(CH_3)_2$), 0.56 (d, 6H, Leusine-*iso*-prop-$(CH_3)_2$); FTIR (KBr/ cm^{-1}): $\nu_{(Ar)C-H}$ 2957, $\nu_{COOassym}$ 1627, ν_{COOsym} 1374, $\Delta\nu_{COO}$ 253.

[Ru(η^6-p-cym)(FcA-4)Cl] **(RAFcA-4)**:

RAFcA-4 was synthesized by reaction of [Ru(η^6-*p*-cymene)Cl_2]$_2$ (0.049 mmol, 30.0 mg) and ligand **FcA-4** (0.098 mmol, 39.4 mg). Soluble in almost all organic solvents like DMSO, MeOH, CH_2Cl_2. Yield: 69.9%; Molecular Weight 673.01 g/mole; Molecular Formula $C_{32}H_{36}ClFeN_2O_2Ru$; Anal. Found: C, 56.83; H, 5.40; N, 3.99. Calc.: C, 57.11; H, 5.39; N, 4.16. ESI-MS *m/z*: 672.9 (M^+), 636.9 (M^+-Cl); δ_H (400 MHz, DMSO-d_6): 11.2 (s, 1H, indolinic N-H of tryptophan), 5.80-5.77 (m, 4H, *p*-cym Ar-H), 4.63 (t, 2H, substituted cyclopentadiene), 4.46 (t, 2H, substituted cyclopentadiene), 4.15 (s, 5H, cyclopentadiene), 2.81 (q, 1H, *p*-cym-*iso*-prop-CH), 2.07 (s, 3H, *p*-cym Ar-CH_3), 1.21 (d, 6H, *p*-cym-*iso*-prop-$(CH_3)_2$); FTIR (KBr/ cm^{-1}): $\nu_{(Ar)C-H}$ 2962, $\nu_{COOassym}$ 1622, ν_{COOsym} 1386, $\Delta\nu_{COO}$ 236.

2.4. *DNA binding experiments*

2.4.1. UV Absorption studies:

The interaction of the complexes with CT DNA has been studied with UV spectroscopy in order to investigate the possible binding modes to CT DNA and to calculate the binding constants (K_b). Absorption studies were performed with fixed complex concentration while varying the CT-DNA concentration within. Stock solutions of the complexes were diluted with tris buffer to get the desired concentration (62.5 µM). While measuring the absorption, equal increments of CT-DNA were added at different ratios to both the complex solution and the reference solution to eliminate the absorbance of CT-DNA itself.

2.4.2. Competitive binding studies with EB using fluorescence spectroscopy:

The competitive binding study with EB has been investigated with fluorescence spectroscopy in order to examine whether each complex can displace EB from DNA–EB complex. The DNA–EB complex was prepared by adding EB (66.6 µM) and DNA (56.5 µM) in tris buffer. The binding mode of complexes **RAFcA 1-4** with CT-DNA was studied by adding a certain amount of a solution of each complex step by step into the solution of the DNA–EB complex. The influence of the addition of each complex has been obtained by recording the variation in the fluorescence emission spectra of the DNA-EB complex. The fluorescence intensities of EB bound to CT-DNA were measured at 609 nm (524 nm excitation) after addition of different concentrations of the complexes at different ratios.

2.5. *BSA binding experiments*

Steady-state fluorescence spectroscopy: The protein-binding study was performed employing steady state fluorescence spectroscopy. Tryptophan fluorescence quenching experiments were carried out using bovine serum albumin (BSA, 16.6 µM) in buffer (containing 15 mM trisodium citrate and 150 mM NaCl at pH 7.0). The quenching of emission intensity of the tryptophan residues of BSA at 343 nm was monitored in the presence of increasing concentrations of complexes **RAFcA 1-4** (0-20 µM) as quenchers [30]. Fluorescence spectra were recorded from 300 to 500 nm at an excitation wavelength of 296 nm.

2.6. *Cytotoxicity*

Standard 3-(4, 5-dimethylthiazole)-2,5-diphenyltetraazolium bromide (MTT) assay was used [31]. MCF7 cells (5.0 x 10^3 cells $well^{-1}$) were placed in 96-well culture plates (Tarson India Pvt. Ltd.) and grown overnight at 37°C in a 5% CO_2 incubator. Compounds to be tested were then added to the wells to achieve final concentrations ranging from 20-100 µg/ml. Control wells were prepared by addition of culture medium without the compounds. The plates were incubated at 37°C in a 5% CO_2 incubator for 24 h. Upon completion of the incubation, MTT dye solution (prepared using serum free culture medium) was added to each well to a final concentration of 0.5 mg/ml. After 4 h of incubation with MTT, the culture media was discarded and the wells were washed with Phosphate Buffer Saline (Hi-Media, India Pvt. Ltd.), followed by addition of DMSO to dissolve the formazan crystals so formed and subsequent incubation for 30 min. The optical density of each well was measured spectrophotometrically at 563 nm using Biotek-ELX800MS universal ELISA reader (Bio-Tek instruments, Inc., Winooski, VT). The IC_{50} values were determined by plotting the percentage viability *versus* concentration on a logarithmic graph and reading off the concentration at which 50% of cells remained viable relative to the control. Each experiment was repeated at least three times to obtain mean values.

2.7. *Gene expression studies*

Expression of apoptosis related genes, Bax (pro-apoptotic) and Bcl-2 (anti-apoptotic) were studied using Real Time PCR (RT-PCR) wherein GAPDH was used as a control. The studies were carried out on A549 and MCF7 cell lines. The IC_{50} values from MTT assay was taken as dosage for the treatment. Total RNA was isolated using TRIzol reagent (Invitrogen, California, USA). cDNA was synthesized by reverse transcription of 1 µg of total RNA using iScript cDNA Synthesis kit (BIORAD, California, USA). PCR was carried out using SYBR Green Master Mix kit (Invitrogen, California, USA) according to manufacturer's instruction. Cycler conditions were as follows: Initial denaturation at 95°C for 3 min further it was followed by 35 reaction cycles (30 sec at 94°C, 30 sec at 55°C and 30 sec at 72°C) and final cycle at 72°C for 10 min. Statistical analysis was done by using One way ANOVA. Primers used for this study are listed in **Table 1**.

Table 1: *Primers used for gene expression study*

List of genes	*Details*	*Length of amplicon*
GAPDH	Accession number (NM_002046) Forward primer (Template: 113-132) 5′-GCTCTCTGCTCCTCCTGTTC-3′ Reverse primer (Template: 366-385) 5′-CAGTTCCGACTCTTGCCCT -3′	273bp
Bcl-2	Accession number (NM_000633) Forward primer (Template: 959-978) 5′-GTCATGTGTGTGGAGAGCGT-3′ Reverse primer (Template: 1083-1102) 5′-GGAAACACCTTGACATGCCG -3′	144bp
BAX	Accession number (NM_001291428) Forward primer (Template: 138-157) 5′-GGCCCTTTTGCTTCAGGGTT -3′ Reverse primer (Template: 341-360) 5′-AGAAAAAGGCTCACCGTCGA-3′	223bp

3. Results and discussion

3.1. *Characterization*

3.1.1. Mass spectrometry:

The ESI-MS spectra of the complexes **RAFcA 1-4** showed molecular ion peaks at *m/z* values equivalent to their molecular weights. The *m/z* values of all the complexes are in well agreement with the proposed composition (**scheme1**) and have been tabulated in **Table 2**. All the mass spectra have been provided as supplementary material **Fig. S1**. Furthermore the composition and purity of the complexes have been confirmed by their C, H, N elemental analysis.

Table 2: *m/z values of complexes* ***RAFcA 1-4*** *showing fragmentation.*

Compound	*m/z values*	*Fragments*
RAFcA-1	650.1	$[Ru(\eta^6\text{-}p\text{-cym})(FcA\text{-}1)Cl]^+ +1$ (M^++1)
	614.1	$[Ru(\eta^6\text{-}p\text{-cym})(FcA\text{-}1)]^+$ (M^+-Cl)
RAFcA-2	633.9	$[Ru(\eta^6\text{-}p\text{-cym})(FcA\text{-}2)Cl]^+$ (M^+)
	597.9	$[Ru(\eta^6\text{-}p\text{-cym})(FcA\text{-}2)]^+$ (M^+-Cl)
RAFcA-3	599.9	$[Ru(\eta^6\text{-}p\text{-cym})(FcA\text{-}3)Cl]^+$ (M^+)
	563.9	$[Ru(\eta^6\text{-}p\text{-cym})(FcA\text{-}3)]^+$ (M^+-Cl)
RAFcA-4	672.9	$[Ru(\eta^6\text{-}p\text{-cym})(FcA\text{-}4)Cl]^+$ (M^+)
	636.9	$[Ru(\eta^6\text{-}p\text{-cym})(\ FcA\text{-}4)]^+$ (M^+-Cl)

3.1.2. FTIR spectroscopy:

The IR spectra of the complexes **RAFcA 1-4** displayed characteristic strong stretching bands at 1580-1630 cm^{-1} and weaker bands at 1370-1395 cm^{-1} due to asymmetric and symmetric carboxylate (COO^-) stretch respectively which were found as strong bands in the fingerprint region at 1580-1610 cm^{-1} in the spectra of free ligands **FcA 1-4** [28]. The separation frequency Δν values fall in the range 188–255 cm^{-1} indicating a monodentate coordination mode of the carboxylato group of the ligand to the metal [32, 33]. The distinct broad band at ~3450 cm^{-1} owing to the O-H stretching of free carboxylic acid group found in the ligand is completely lost in the IR spectra of the complex indicating complexation of the ligand with metal via the carboxylate oxygen. Furthermore the medium secondary amine N-H stretching bands in the spectra of the free ligands in the region of 2900-3000 cm^{-1} were found to have positive shifts in the region of 3050-3200 cm^{-1} in complexes indicating complexation of the ligand with metal via the nitrogen of secondary amine (mannich base). The presence of weak to medium bands in the fingerprint regions 2900-3000 cm^{-1} owing to aromatic $\nu_{C\text{-}H}$ stretch and strong bands around 1430-1667 cm^{-1} due to the aromatic $\nu_{C=C}$ in plane vibrations is indicative of presence of *p*-cymene in the complex.

3.1.3. Electronic spectra:

The electronic absorption spectra of the complexes **RAFcA 1-4** recorded in DMSO solution showed absorption bands in the region 200-500 nm. The electronic spectra of free ligands **FcA 1-4**

displayed intense absorption bands at 207-209 nm ascribable to intra ligand π→π* transition of the cyclopentadienyl rings of ferrocene [28] which were observed to have shifted to longer wavelength region at 260-280 nm (**Fig. 2**) due to coordination with Ru(II) metal centre. All the four complexes showed broad shoulder peaks in the region 300-340 nm corresponding to *n*→π* transitions, whereas the MLCT transitions have been obtained as broad peaks in the region 370-420 nm. The absorption peak values have been tabulated in **Table 3**.

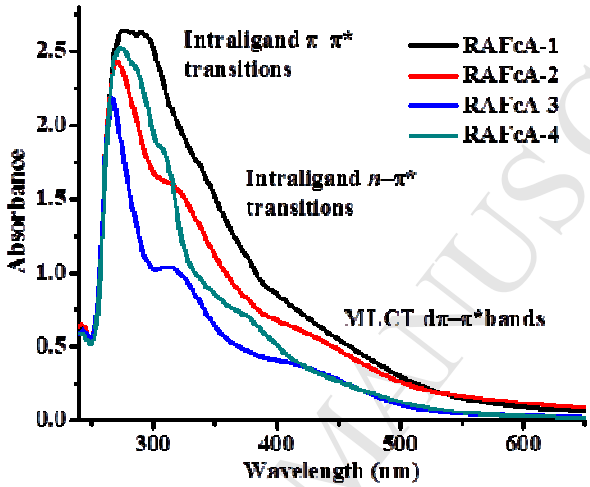

Fig. 2: *UV-vis. spectra of complexes* ***RAFcA 1-4*** *recorded in DMSO with path length 1 cm.*

Table 3: *UV-Vis. peak assignments of* ***RAFcA 1-4***

Compound	*Intra-ligand transitions (nm)*		*MLCT dπ-π* transitions (nm)*
	*π-π**	*n-π**	
RAFcA-1	277	336	-
RAFcA-2	271	318	407
RAFcA-3	266	316	420
RAFcA-4	274	308	373

3.1.4. Powder X-ray diffraction:

The PXRD for the complexes **RAFcA-1** and **RAFcA-2** within the 2θ range 5-50 show many sharp peaks which provide a clear evidence of the crystalline nature of the compounds (**Fig. S2**).

3.2. *DNA binding studies*

3.2.1. Electronic absorption titration:

The presence of ground state interactions between the biological macromolecule DNA and compounds under study have been detected using absorption spectroscopy. DNA can provide three distinctive binding sites (groove binding outside of DNA helix, along major or minor groove, electrostatic binding to phosphate group and intercalation), a behavior important for the biological role of antibiotic and anticancer drugs *in vivo* [34]. The binding efficiency of metal complex to DNA can be effectively investigated employing electronic spectroscopy since the observed changes in the spectra may give evidence of the existing interaction mode [35]. Any interaction between the compounds and DNA is expected to perturb the ligand centered transitions of the compounds. Binding with DNA via non-intercalative binding modes, such as electrostatic forces, van der Waals interactions, dative bonds, hydrogen bonds and hydrophobic interactions generally results in increase in absorption intensity (hyperchromism) upon increasing the concentration of CT-DNA owing to the degradation of the DNA double helix structure. On the other hand intercalation generally results in hypochromism and a red shift (bathochromism) of the absorption band due to a strong stacking interaction between an aromatic moiety of the ligand and the base pairs of the DNA [36, 37]. The UV spectra of complexes **RAFcA 1-4** have been recorded in absence and presence of varying CT-DNA concentration (0-100 µM) within. The absorption bands of the complexes (**Fig**. **3**) centered at 207-208 nm showed significant hypochromism and a slight red shift. DNA intercalators show a much larger bathochromic shift and hypochromism of the spectral bands, although the intercalative mode of binding of the complexes with DNA cannot be ruled out completely [38].

The magnitude of binding strength to CT-DNA may be determined through the calculation of binding constant K_b which is obtained by monitoring the changes in the absorbance of the compounds with increasing concentrations of CT-DNA. K_b is given by the ratio of slope to the y intercept in the plots [DNA]/(ε_A-ε_f) versus [DNA] (**Fig. 3, *inset)*** according to eq. **(1)** [39]

$$\mathbf{[DNA]/(\varepsilon_A-\varepsilon_f) = [DNA]/(\varepsilon_b-\varepsilon_f)+1/K_b(\varepsilon_b-\varepsilon_f)} \qquad \mathbf{(1)}$$

where [DNA] is the concentration of DNA in base pairs, $\varepsilon_A = A_{obsd}/$ [compound], ε_f is the extinction coefficient for the unbound compound (**RAFcA 1-4**) and ε_b is the extinction coefficient for the compound in the fully bound form. The binding constant K_b values (**Table 4**) for the complexes are in the range of 2.1 - 3.9 x 10^3 M^{-1} indicative of moderate binding to DNA. Complex **RAFcA-1** with a tyrosine substituted ferrocenyl moiety bound to the Ru(II) centre shows the highest binding constant value due to additional hydrogen bonding interactions between –OH group of tyrosine and DNA nucleobases which are accessible both in major groove and minor groove. The titration curves for the remaining complexes **RAFcA 2-4** have been provided as supplementary material in **Fig. S3**

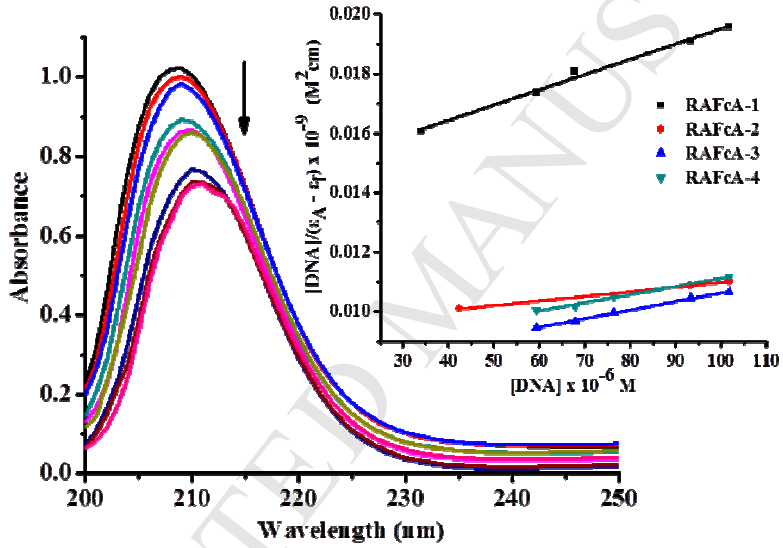

Fig. 3: *UV absorption spectra of **RAFcA-1** at increasing concentrations of CT-DNA, the arrow shows decrease in intensity upon increasing concentration of the DNA. Inset: Plot of [DNA]/(ε_A -ε_f) versus [DNA] for **RAFcA 1-4**.*

3.2.2. Competitive binding studies with Ethidium Bromide using fluorescence spectroscopy:

Ethidium Bromide (=3,8-diamino-5-ethyl-6-phenyl-phenanthridinium bromide) is a phenanthridine fluorescence dye and is a typical indicator of intercalation, forming soluble complexes with nucleic acids and emitting intense fluorescence in the presence of CT DNA due to the intercalation of the planar phenanthridinium ring between adjacent base pairs on the double helix [40, 41]. Addition of a second molecule, which may bind to DNA more strongly than EB results in a

decrease of the DNA-induced EB emission [42]. The emission spectra of DNA-EB (λ_{ex} = 546 nm, λ_{em} = 610) in the absence and presence of increasing amounts of complexes have been recorded. Addition of complexes resulted in a significant decrease of the intensity of the emission band at 609 nm indicating the competition of the compounds with EB in binding to DNA (**Fig. 4**). The observed quenching of DNA–EB fluorescence suggests that they displace EB from the DNA–EB complex and interact with DNA by intercalation.

The relative binding of complexes to CT-DNA was determined by calculating the quenching constant (K_{SV}) from the slopes of straight lines obtained from the Stern-Volmer equation **(2)** [43]:

$$\mathbf{Io/I = 1 + K_{SV}[Q]} \qquad \mathbf{(2)}$$

where Io and I are the emission intensities in the absence and the presence of the quencher **RAFcA 1-4** respectively, [Q] is the concentration of the quencher and K_{SV} is the Stern–Volmer constant which can be obtained from the slope of the plot of Io/I *versus* [Q].

The Stern–Volmer quenching plots (**Fig. 4, *inset***) illustrate that the quenching of EB bound to DNA is in good agreement (R = 0.93-0.99) with the linear Stern–Volmer equation and the Stern-Volmer quenching constant K_{SV} values are given in **Table 4.** Complexes **RAFcA-1** and **4** show higher quenching constant values of 4.7 x 10^3 M^{-1} and 4.0 x 10^3 M^{-1} respectively indicating their greater efficiency to replace EB and bind strongly with DNA which is also evident from their higher DNA binding constant (K_b) values. The titration curves for rest of the complexes have been provided as supplementary material in **Fig. S4**.

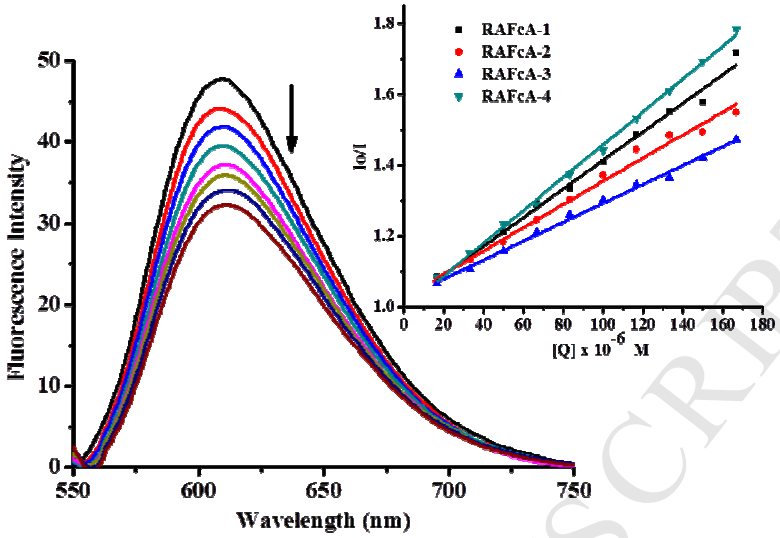

Fig. 4: *Fluorescence emission spectra of DNA-EB complex at increasing concentrations of* ***RAFcA-1****, the arrow shows decrease in intensity upon increasing concentration of the complex. Inset: Stern-Volmer quenching plot* I_0/I *versus [Q] of DNA-EB for* ***RAFcA 1-4****.*

Table 4: *DNA binding constants of* ***RAFcA 1-4****.*

Compound	***DNA binding constants***		
	$K_b\ M^{-1}$	$K_{SV}\ M^{-1}$	***λ shift***
RAFcA-1	3.9×10^3	4.0×10^3	3 nm
RAFcA-2	2.1×10^3	3.3×10^3	5 nm
RAFcA-3	3.4×10^3	2.7×10^3	4 nm
RAFcA-4	3.5×10^3	4.7×10^3	4 nm

3.3. *BSA binding studies*

Steady-state fluorescence spectroscopy: BSA is extensively studied, due to its structural homology with human serum albumin (HSA). HSA contains one tryptophan located at position 214, while BSA has two tryptophan residues at positions 134 and 212 along the chain. BSA solutions exhibit a strong fluorescence emission with a peak at 343 nm, due to the tryptophan residues, when excited at 296 nm [30, 44]. The complexes did not show any emission in the range 300-450 nm on excitation at 296 nm. Addition of increasing concentrations of the complexes to a solution of BSA results in a decrease of the fluorescence intensity as shown for **RAFcA-1** in **Fig. 5** because of their binding to BSA which may change the protein conformation, subunit association or denaturation leading to changes in the tryptophan environment of BSA. In case of **RAFcA-4**, the titration plot with BSA shows a new peak being formed at 453 nm with increasing complex concentration (**Fig. S5c**). This new peak is due to the intrinsic fluorescence of the complex owing to the tryptophan moiety attached to the ferrocene.

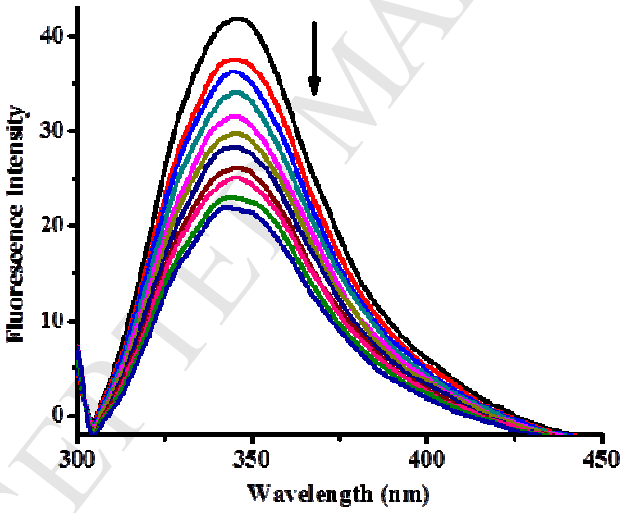

Fig. 5: *Fluorescence emission spectra of BSA at increasing concentrations of* ***RAFcA-1****, the arrow shows decrease in intensity upon increasing concentration of the complex.*

The values of the Stern–Volmer quenching constant (K_{SV} M^{-1}) and the quenching rate constant (kq, M^{-1} s^{-1}) for the the complexes **RAFcA 1-4** interacting with BSA as calculated by Stern-Volmer quenching equation (Eq. **2**) and the corresponding Stern-Volmer plots (**Fig**. **6a**) are cited in **Table 5** which suggest

good binding propensity of the complexes with BSA [45]. The titration curves for complexes **RAFcA 2-4** are provided as supplementary material in **Fig. S5.**

The association binding constant K_a (M^{-1}) and the number of binding sites per albumin (*n*) can be calculated by double logarithm equation (Eq.**3**) [46]

$$\log (Io-I)/I = \log K_a + n \log [Q] \quad (3)$$

The plot of log [(Io-I)/I] versus log [Q] for all the ligands and complexes are linear (**Fig. 6b**) and the K_a and *n* values for the complexes have been obtained from the intercept and slope, respectively (**Table 5**).

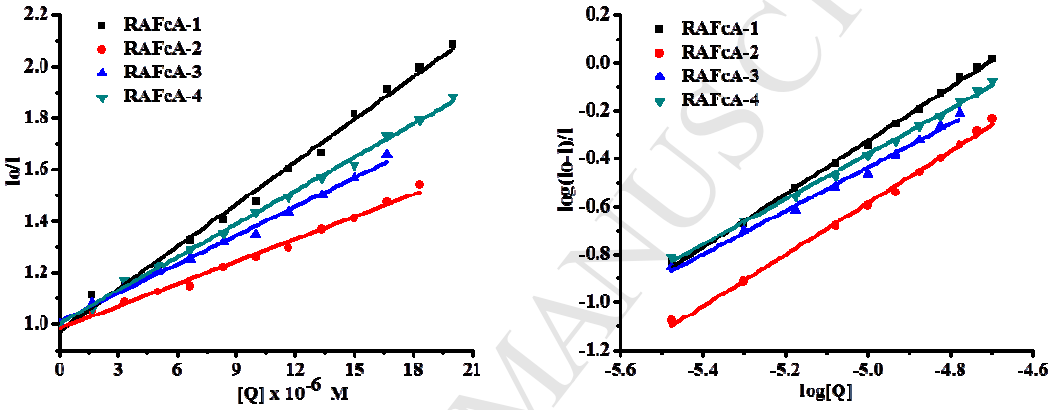

(a) **(b)**

Fig. 6: (a) *Stern volmer plots and* ***(b)*** *Double logarithmic plot for the quenching of BSA fluorescence by* ***RAFcA1-4***

Table 5: *BSA binding constants of* ***RAFcA 1-4***

Compound	*BSA binding constants*		
	$K_a\ M^{-1}$	$K_{SV}\ M^{-1}$	*n*
RAFcA-1	1.7×10^5	5.4×10^4	1.1
RAFcA-2	6.5×10^4	2.8×10^4	1.1
RAFcA-3	1.2×10^6	3.7×10^4	0.9
RAFcA-4	2.3×10^4	4.3×10^4	0.9

In general, the values of association binding constants (K_a) suggest good binding propensities of the complexes to BSA. The *n* values for the complexes average out to be 1 which suggests that there is only one binding site available on the protein. Moreover the linear nature of the double logarithm plots of **RAFcA 1-4** indicates that only one of the tryptophan residues on BSA protein is interacting with the compounds [47].

3.4. *Cytotoxicity*

In-vitro cytotoxicity tests were performed on the human breast carcinoma (MCF7) cell line. The cell viabilities (%), obtained for MCF7 cells with continuous exposure to the complexes for 48 h, are depicted in **Fig. 7**. The cytotoxicities were found to be dose dependent, that is, the cell viability decreased with increasing concentrations of the complexes. The IC_{50} values of the complexes have been tabulated in **Table 6**. The reported IC_{50} values of NAMI-A, which is a well known ruthenium complex currently under phase 2 clinical trials, have been found to be in the range of 550-750 µM for various cancer cell lines on treatment for 48 h [48, 49] and >1600 µM for RAPTA, a well studied ruthenium- arene complex, for MCF7 cell line on treatment for 72 h [50]. Although the synthesized ruthenium complexes are found to be less active compared to *cis* platin (IC_{50} = 26 µM), they are much more active on cancer cells as compared to NAMI-A with **RAFcA-4** (IC_{50} = 37.1 µM) showing the maximum potency.

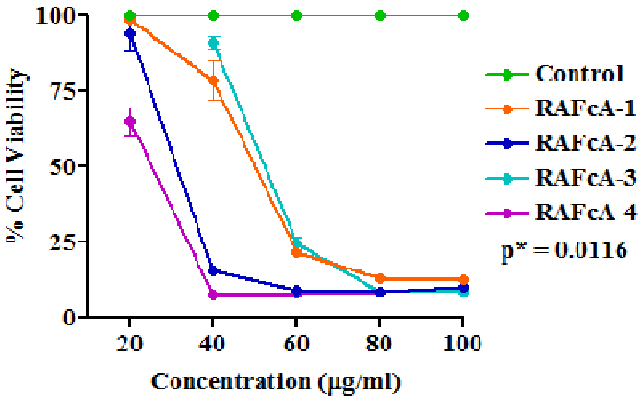

Fig. 7 *% Cell viability in presence of complexes* ***RAFcA 1-4*** *for MCF7 human breast cancer cell lines. Each point is the mean ± standard error obtained from three independent experiments.*

Table 6: *IC_{50} values of complexes* ***RAFcA 1-4*** *obtained from MTT assay on MCF7 cells.*

Compound	***IC_{50} values***	
	µg/ml	***µM***
RAFcA-1	49 (±3.85)	75.5
RAFcA-2	30 (±3.23)	47.3
RAFcA-3	52 (±1.11)	86.6
RAFcA-4	25 (±2.69)	37.1

3.5. *Gene expression studies:*

Expression levels of pro-apoptotic (Bax) and anti-apoptotic (Bcl-2) genes were assessed on MCF7 (human breast carcinoma) by 48 h exposure of a ruthenium(II)arene complex to the cancer cells. The complex **RAFcA-4** with the lowest IC_{50} value (25µg/ml) has been selected for the gene expression studies. Results (**Fig. 8**) revealed that the expression of Bax notably increased after treatment with the complex suggesting that it possibly has capacity to trigger apoptotic pathway and cause death of cancer cells. Alternatively expression levels of Bcl-2 in the cancer cells treated with the complex were significantly low further suggesting higher vulnerability for trigger of apoptosis. These results provide valuable evidence on the role of the synthesized complexes in triggering apoptosis in cancer cells and indicate towards the merits of Ru(II)-arene complexes as potent anticancer agents.

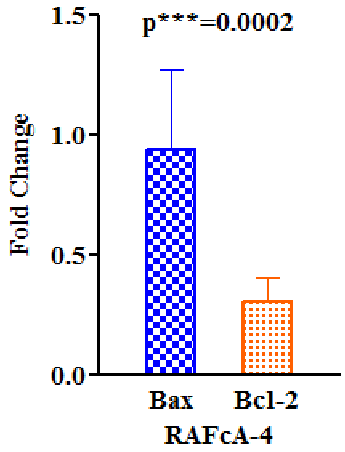

Fig. 8: *Expression levels of pro-apoptotic gene (Bax) and anti-apoptotic gene (Bcl-2) were studied using quantitative real time PCR. The CT values were determined and transformed into fold change in expression. Statistical analysis was done using One way Anova, for n=2, p<0.0002****

4. Conclusion

The work discussed here thus focuses on the synthesis, characterization and bioactivity of the ruthenium complexes [Ru(η^6-*p*-cym)(L)Cl] where L = ferrocenyl amino acid mannich base conjugates. Literature has already shown that ferrocenyl compounds are good DNA and protein binders which in the present study have been found to be further enhanced on complexation with ruthenium. This can be based on their better binding constants obtained for interactions with DNA and BSA compared to those of the free ligands [28]. Moreover the mixed ligand Ru(II)-arene complexes show intercalative mode of binding to DNA unlike the ferrocenyl mannich base ligands which were found to be good groove binders [28]. Such impressive binding efficacies of the ruthenium complexes containing ferrocenyl amino acids broaden their scope for *in-vitro* investigations as potent anticancer agents following which we carried out the cytotoxicity studies employing MTT assay. Lower IC_{50} values of the complexes, can be attributed to the presence of a hydrophobic arene moiety which facilitates cellular uptake of the complexes. Furthermore the mode of cell death, scrutinized by gene expression studies was found to be apoptosis also called as programmed cell death which is the preferred mode of cell death over necrosis.

Acknowledgement

The authors gratefully acknowledge the University Grants Commission [RFSMS-BSR fellowship], New Delhi, for their financial assistance. The authors are thankful to the Head, Department of Chemistry and Department of Zoology, Faculty of Science, The Maharaja Sayajirao University of Baroda for providing the necessary lab facilities and required instrumentation facilities to carry out the research work. The authors thank DBT-MSUB-ILSPARE project, Dr. Vikram Sarabhai Science Block, The M.S. University of Baroda for providing the facility to carry out gene expression studies.

References

[1] B. Christophe, F. Nadine, M. Lucien, B. Jacques, P. Daniel, Bioorg. Med. Chem. Lett. 10 (2000) 839-841.

[2] R. Epton, G. Marr, G.K. Rogers, J. Organomet. Chem. 110 (1976) 42-44.

[3] B. Christophe, D. Laurence, A.M. Lucien, M. Marlène, C. Daniel, S.B. Jacques, Eur. J. Med. Chem. 35 (2000) 707-714.

[4] B. Francois, C. Frederic, V. Laure, B. Jacques, M. Bernard, R. Anne, J. Med. Chem. 53 (2010) 4103-4109.

[5] A. Ion; J. Moutet; E. Saint-Aman, G. Royal, I. Gautier- Luneau, M. Bonin, R. Ziessel, Eur. J. Inorg. Chem. 6 (2002) 1357-1366.

[6] L.J. Kuo, J.H. Liao, C.T. Chen, C.H. Huang, C.S. Chen, J.M. Fang, Org. Lett. 5 (2003) 1821-1824.

[7] J. Westwood, S.J. Coles, S.R. Collinson, G. Gasser, S.J. Greem, M.B. Hursthouse, M.E. Light, J.H. Tucker, Organometallics 23 (2004) 946-951.

[8] M. Inouye, Y. Hyodo, H. Nakazumi, J. Org. Chem. 64 (1999) 2704-2710.

[9] M. Takase, M. Inouye, J. Org. Chem. 68 (2003) 1134-1137.

[10] P. Debroy, M. Banerjee, M. Prasad, S.P. Moulik, S. Roy, Org. Lett. 7 (2005) 403-406.

[11] K. Seio, M. Mizuta, T. Terada, M. Sekine, J. Org. Chem. 70 (2005) 10311-10322.

[12] (a) R. Gul, M.K. Rauf, A. Badshah, S.S. Azam, M.N. Tahir, A. Khan, Eur. J. Med. Chem. 85 (2014) 438-449.
(b) S. Hussain, A. Badshah, B. Lal, R.A. Hussain, S. Ali, M.N. Tahir, A.A. Altaf, J. Coord. Chem. 67 (2014) 2148-2159.

(c) T.K. Goswami, S. Gadadhar, M. Roy, M. Nethaji, A.A. Karande, A.R. Chakravarty, Organometallics 31 (2012) 3010-3021.

[13] A.M. Gellett, P.W. Huber, P.J. Higgins, J. Organomet. Chem. 693 (2008) 2959–2962.

[14] P.J. Higgins, A.M. Gellett, Bioorg. Med. Chem. Lett. 19 (2009) 1614–1617.

[15] (a) S. Top, A. Vessières, G. Leclercq, J. Quivy, J. Tang, J. Vaissermann, M. Huché, G. Jaouen, Chem. A Eur. J. 9 (2003) 5223-5236;

(b) G. Jaouen, S. Top, A. Vessières, G. Leclercq, M.J. McGlinchey, Curr. Med. Chem. 11 (2004) 2505-2517;

(c) A. Vessières, S. Top, P. Pigeon, E. Hillard, L. Boubeker, D. Spera, G. Jaouen, J. Med. Chem. 48 (2005) 3937-3940;

(d) E. Hillard, A. Vessières, L. Thouin, G. Jaouen, C. Amatore, Angew. Chem. Int. Ed. 45 (2006) 285-290;

(e) A. Vessieres, S. Top, W. Beck, E. Hillard, G. Jaouen, Dalton Trans. 4 (2006) 529-541;

(f) A. Nguyen, E.A. Hillard, A. Vessières, S. Top, P. Pigeon, G. Jaouen, Chimia 61 (2007) 716-724;

(g) O. Buriez, J.M. Heldt, E. Labbé, A. Vessières, G. Jaouen, C.Amatore, Chem. A Eur. J. 14 (2008) 8195-8203;

(h) Q.Michard, G. Jaouen, A. Vessieres, B.A. Bernard, J. Inorg. Biochem. 102 (2008) 1980-1985;

(i) P. Pigeon, S. Top, O. Zekri, E.A. Hillard, A. Vessières, M.-A. Plamont, O. Buriez, E. Labbé, M. Huché, S. Boutamine, C. Amatore, G. Jaouen, J. Organomet. Chem. 694 (2009) 895-901;

(j)M.Gormen,D.Plazuk, P. Pigeon, E.A.Hillard,M.-A. Plamont, S. Top,A.Vessières, G. Jaouen, Tetrahedron Lett. 51 (2010) 118-120.

[16] C. Ornelas, New J. Chem. 35 (2011) 1973–1985.

[17] P. J. Dyson, Chimia 61 (2007) 698-703.

[18] S. J. Dougan, P. J. Sadler, Chimia 61 (2007) 704-715.

[19] L. D. Dale, J. H. Tocher, T. M. Dyson, D. I. Edwards, A. Tocher, Anti-Cancer Drug Design 7 (1992) 3-14.

[20] S. J. Dougan, M. Melchart, A. Habtemariam, S. Parsons, P. J. Sadler, Inorg. Chem. 45 (2006) 10882-10894.

[21] F. Wang, A. Habtemariam, E. P. L. van der Geer, R. Fernandez, M. Melchart, R. J. Deeth, R. Aird, S. Guichard, F. P. A. Fabbiani, P. Lozano-Casal, I. D. H. Oswald, D. I. Jodrell, S. Parsons, P. J. Sadler, Proc. Natl. Acad. Sci. U.S.A. 102 (2005) 18269-18274.

[22] A. M. Pizarro, H. Abraha, P. J. Sadler, Top. Organomet. Chem. 32 (2010) 21-56.

[23] J. Prousek, Pure Appl. Chem. 79 (2007) 2325–2338.

[24] J. Tauchman, G. Süss-Fink, P. Stepnicka, O. Zava, P.J. Dyson, J. Organomet. Chem. 723 (2013) 233-238.

[25] T.M. Sielecki, J.F. Boylan, P.A. Benfield, G.L. Trainor, J. Med. Chem. 43 (1999) 1–18.

[26] Z. Zang, L. Jin, X. Qian, M. Wei, Y. Wang, J. Wang, Y. Yang, Q. Xu, Y. Xu, F. Liu, ChemBioChem. 8 (2007) 113–121.

[27] P.K.M. Siu, D.L. Ma, C.M. Che, Chem. Commun. (2005) 1025–1027.

[28] P. Ramadevi, R. Singh, S. S. Jana, R. Devkar, D. Chakraborty, J. Photochem. Photobiol. : Part A 305 (2015) 1-10.

[29] M. A. Bennett, A. K. Smith, J. Chem. Soc. Dalton Trans. (1974) 233-241.

[30] J.R. Lakowicz (1999) Principles of Fluorescence Spectroscopy, 2nd edn., Plenum Press, New York

[31] T. Mosmann, J. Immunol. Methods 65 (1983) 55-63.

[32] G. B. Deacon, R. J. Phillips, Coord. Chem. Rev. 33 (1980) 227-250.

[33] G. Gehad, H. F. Mohamed, A. El-Halim, M. I. Maher, W. El-Dessouky, H. Mahmoud, J. Mol. Struct. 999 (2011) 29-38.

[34] J.M. Kelly, A.B. Tossi, D.J. McConnell, Nucleic Acids Res. 13 (1985) 6017-6034.

[35] G. Son, J. Yeo, M. Kim, S. Kim, A. Holmen, B. Akerman, B. Norden, J. Amer. Chem. Soc. 120 (1998) 6451-6457

[36] S. Tabassum, W.M.Al–Asbahy, M. Afzal, Manalshamsi, F. Arjmand, J. of Luminescence, 132 (2012) 3058-3065.

[37] Y.Y. Xie, H.L. Huang, J.H. Yao, G.J. Lin, G.B. Jiang, Y.J. Liu, Eur. J. of Chem. 63 (2013) 603-610.

[38] T.K. Goswami, B.V.S.K. Chakravarthi, M. Roy, A.A. Karande, A.R. Chakravarty, Inorg. Chem. 50 (2011) 8452–8464.

[39] A.M. Pyle, J.P. Rehmann, R. Meshoyrer, C.V. Kumar, N.J. Turro, J.K. Barton, J. Am. Chem. Soc. 111 (1989) 3051-3058.

[40] G. Zhao, H. Lin, S. Zhu, H. Sun, Y. Chen. J. Inorg. Biochem. 70 (1998) 219-226.

[41] S. Dhar, M. Nethaji, A.R. Chakravarty. J. Inorg. Biochem. 99 (2005) 805-812.

[42] R.F. Pasternack, M. Cacca, B. Keogh, T.A. Stephenson, A.P. Williams, F.J. Gibbs, J. Am. Chem. Soc. 113 (1991) 6835-6840.

[43] J.R. Lakowicz, G. Weber, Biochemistry 12 (1973) 4161-4170.

[44] Y. Wang, H. Zhang, G. Zhang, W. Tao, S. Tang, J. Luminescence 126 (2007) 211-218.

[45] S.H. Lai, W. Li, X.Z. Wang, C. Zhang, C.C. Zeng, B. Tang, D. Wan, Y.J. Liu, RSC Adv. 6 (2016) 63143-63155.

[46] B. Ahmad, S. Parveen, R.H. Khan, Biomacromolecules 7 (2006) 1350–1356.

[47] B. Mishra, A. Barik, K.I. Priyadarsini, H. Mohan, J. Chem. Sci. 117 (2005) 641–647.

[48] H. Petra, K. Bock, B. Atil, M. A. Hoda, W. Korner, C. Bartel, U. Jungwirth, B. K. Keppler, M. Michael, W. Berger, K. Gunda, J. Biol. Inorg. Chem. 15 (2010) 737-748.

[49] C. Tan, S. Hu, J. Liu, J. Liangnian, Eur. J. Med. Chem. 46 (2011) 1555-1563.

[50] H. A. Wee, D. Elisa, S. Claudine, S. Rosario, J. Lucienne, P. J. Dyson, Inorg. Chem. 45 (2006) 9006-9013.

Mixed ligand Ruthenium arene complexes containing N-Ferrocenyl amino acids: Biomolecular interactions and Cytotoxicity against MCF7 cell line

Pulipaka Ramadevi [1], Rinky Singh[1], Sarmita S Jana[2], Ranjitsinh Devkar[2] and Debjani Chakraborty[1*]

[1]Department of Chemistry, Faculty of Science, The M.S. University of Baroda, Vadodara-390002, Gujarat. INDIA.

[2]Division of Phytotherapeutics and Metabolic Endocrinology, Department of Zoology, Faculty of Science, The M.S. University of Baroda, Vadodara-390002, Gujarat. INDIA.

*Corresponding author. Tel.:+91 9537521703, E-mail address: debchak23@gmail.com

Highlights:

- [Ru(η^6-*p*-cym)(L)Cl] where L=N-ferrocenyl amino acid conjugates have been synthesized and explored as anticancer agents..
- DNA and BSA binding has been established by UV-vis and fluorescence studies.
- [Ru(η^6-*p*-cym)(L)Cl] complexes show better cytotoxic activity than NAMI-A and RAPTA
- Fluorescence staining methods and gene expression studies confirm apoptosis induced cell death.